

## A Linear Tetranuclear Single-Molecule Magnet of $\text{Mn}^{\text{II}}\text{Mn}^{\text{III}}_2$ with the Anion of 2-(Hydroxymethyl)pyridine

Dacheng Li,<sup>†</sup> Huisheng Wang,<sup>‡</sup> Suna Wang,<sup>†</sup> Yupeng Pan,<sup>†</sup> Chengjuan Li,<sup>†</sup> Jianmin Dou,<sup>\*,†</sup> and You Song<sup>\*,†</sup>

<sup>†</sup>School of Chemistry and Chemical Engineering, Liaocheng University, 252059 Liaocheng, People's Republic of China, and <sup>‡</sup>State Key Laboratory of Coordination Chemistry, School of Chemistry and Chemical Engineering, Nanjing National Laboratory of Microstructures, Nanjing University, Nanjing, People's Republic of China

Received February 4, 2010

A tetranuclear manganese complex,  $[\text{Mn}_4(\text{hmp})_6(\text{N}(\text{CN})_2)_4(\text{H}_2\text{O})_2]$  (**1**; Hhmp = 2-(hydroxymethyl)pyridine;  $\text{N}(\text{CN})_2^-$  = dicyanamide anion), was synthesized and characterized by single-crystal X-ray diffraction, bond valence sum calculations, IR spectra, elemental analysis, and magnetic measurements. The structure of **1** consists of a linear  $[\text{Mn}^{\text{II}}_2\text{Mn}^{\text{III}}_2]$  core formed by six hmp<sup>−</sup> groups linking  $\text{Mn}^{\text{II/III}}$  ions. Magnetic studies show that **1** behaves as a single-molecule magnet with ferromagnetic coupling between the metal centers.

Manganese clusters have received considerable interest in recent years because some of these can function as single-molecule magnets (SMMs), which show magnetic hysteresis arising from slow magnetization reversal due to a high energy barrier.<sup>1,2</sup> The barrier relates to easy-axis anisotropy [negative zero-field-splitting (ZFS) parameter,  $D$ ] and to the large ground-state spin,  $S$ .<sup>3</sup> Moreover, these compounds exhibit interesting physical phenomena such as quantum tunneling of magnetization, spin-parity effects, spin–spin cross-relaxation, and coherence effects.<sup>4</sup>

In order to obtain new polynuclear clusters, some groups have employed 2-(hydroxymethyl)pyridine (Hhmp) as a

chelate ligand because the alkoxide arm often supports ferromagnetic coupling between the metal atoms.<sup>5c</sup> Up to now, different nuclear manganese clusters based on hmp<sup>−</sup> such as  $\text{Mn}_4$ ,  $\text{Mn}_{12}$ ,  $\text{Mn}_{18}$ ,  $\text{Mn}_{21}$ ,  $\text{Mn}_{25}$ ,  $\text{Mn}_{73}$ , and  $\text{Mn}_{10}$  have been synthesized,<sup>5</sup> and the highest  $S$  is  $61/2$ .<sup>5i</sup> To our knowledge, the former five clusters are rhombus-, rod-, disk-, and barrel-like cage-shaped and show SMM properties; however, the latter two clusters take hexagon and cage shapes without SMM properties owing to extremely low  $D$  values. The reason for the small  $D$  of the latter clusters may be that they possess higher molecular symmetry than the former clusters (for example,  $\text{Mn}_{10}$  possesses tetrahedral symmetry with  $D \approx 0$ ).<sup>5e</sup> Therefore, the lower symmetry clusters such as linear molecules (rather than a 1D chain) would have a larger  $D$ . Herein, we report a rarely linear tetranuclear manganese complex,  $[\text{Mn}_4(\text{hmp})_6(\text{N}(\text{CN})_2)_4(\text{H}_2\text{O})_2]$  (**1**), showing SMM properties (Figure 1).

The reaction of  $\text{MnCl}_2 \cdot 4\text{H}_2\text{O}$ , Hhmp,  $\text{NaN}(\text{CN})_2$ , and  $\text{Et}_4\text{NOH}$  in a 2:5:5:1 molar ratio in  $\text{MeOH}/\text{CH}_3\text{CN}$  (1:2, v/v) gave a dark-red solution, which afforded dark-red single crystals of complex **1** in 35% yield.<sup>6</sup>

\*To whom correspondence should be addressed. E-mail: jmdou@lccu.edu.cn (J.D.), yousong@nju.edu.cn (Y.S.).

(1) Christou, G.; Gatteschi, D.; Hendrickson, D. N.; Sessoli, R. *MRS Bull.* **2000**, 25, 66.

(2) (a) Sessoli, R.; Gatteschi, D.; Caneschi, A.; Novak, M. A. *Nature* **1993**, 365, 141. (b) Sessoli, R.; Tsai, H.-L.; Schake, A. R.; Wang, S.; Vincent, J. B.; Folting, K.; Gatteschi, D.; Christou, G.; Hendrickson, D. N. *J. Am. Chem. Soc.* **1993**, 115, 1804. (c) Gatteschi, D.; Sessoli, R. *Angew. Chem., Int. Ed.* **2003**, 42, 268. (d) Aromil, G.; Brechin, E. K. *Struct. Bonding (Berlin)* **2006**, 122, 1. (e) Goldberg, D. P.; Caneschi, A.; Delfs, C. D.; Sessoli, R.; Lippard, S. J. *J. Am. Chem. Soc.* **1995**, 117, 5789.

(3) (a) Ruiz, D.; Sun, Z.; Albela, B.; Folting, K.; Ribas, J.; Christou, G.; Hendrickson, D. N. *Angew. Chem., Int. Ed.* **1998**, 37, 300. (b) Ako, A. M.; Hewitt, I. J.; Mereacre, V.; Clérac, R.; Wernsdorfer, W.; Anson, C. E.; Powell, A. K. *Angew. Chem., Int. Ed.* **2006**, 45, 4926. (c) Oshio, H.; Nakano, M. *Chem.—Eur. J.* **2005**, 11, 5178.

(4) (a) Hill, S.; Edwards, R. S.; Aliaga-Alcalde, N.; Christou, G. *Science* **2003**, 302, 1015. (b) Wernsdorfer, W.; Bhaduri, S.; Boskovic, C.; Christou, G.; Hendrickson, D. N. *Phys. Rev. B* **2002**, 65, 180403. (c) Wernsdorfer, W.; Bhaduri, S.; Tiron, R.; Hendrickson, D. N.; Christou, G. *Phys. Rev. Lett.* **2002**, 89, 197201. (d) Wernsdorfer, W.; Sessoli, R. *Science* **1999**, 284, 133.

(5) For example, see: (a) Lecren, L.; Wernsdorfer, W.; Li, Y.-G.; Roubeau, O.; Miyasaka, H.; Clérac, R. *J. Am. Chem. Soc.* **2005**, 127, 11311. (b) Miyasaka, H.; Nakata, K.; Lecren, L.; Coulon, C.; Nakazawa, Y.; Fujisaki, T.; Sugiura, K.-I.; Yamashita, M.; Clérac, R. *J. Am. Chem. Soc.* **2006**, 128, 3770. (c) Yoo, J.; Brechin, E. K.; Yamaguchi, A.; Nakano, M.; Huffman, J. C.; Maniero, A. L.; Brunel, L.-C.; Awaga, K.; Ishimoto, H.; Christou, G.; Hendrickson, D. N. *Inorg. Chem.* **2000**, 39, 3615. (d) Harden, N. C.; Bolcar, M. A.; Wernsdorfer, W.; Abboud, K. A.; Streib, W. E.; Christou, G. *Inorg. Chem.* **2003**, 42, 7067. (e) Stamatatos, T. C.; Poole, K. M.; Abboud, K. A.; Wernsdorfer, W.; O'Brien, T. A.; Christou, G. *Inorg. Chem.* **2008**, 47, 5006. (f) Stamatatos, T. C.; Abboud, K. A.; Wernsdorfer, W.; Christou, G. *Angew. Chem., Int. Ed.* **2006**, 45, 4134. (g) Boskovic, C.; Brechin, E. K.; Streib, W. E.; Folting, K.; Hendrickson, D. N.; Christou, G. *Chem. Commun.* **2001**, 467. (h) Sañudo, E. C.; Brechin, E. K.; Boskovic, C.; Wernsdorfer, W.; Yoo, J.; Yamaguchi, A.; Concolino, T. R.; Abboud, K. A.; Rheingold, A. L.; Ishimoto, H.; Hendrickson, D. N.; Christou, G. *Polyhedron* **2003**, 22, 2450. (i) Stamatatos, T. C.; Abboud, K. A.; Wernsdorfer, W.; Christou, G. *Angew. Chem., Int. Ed.* **2007**, 46, 884.

(6) Anal. Calcd for  $\text{Mn}_4\text{C}_{44}\text{H}_{40}\text{N}_{18}\text{O}_8$ : C, 45.18; H, 3.42; N, 21.56. Found: C, 45.10; H, 3.52; N, 21.61. Selected IR (KBr,  $\text{cm}^{-1}$ ): 3386(w), 2299(s), 2241(s), 2155(s), 1604(s), 1569(m), 1480(s), 1436(m), 1384(s), 1358(s), 1289(m), 1253(w), 1224(w), 1071(s), 920(w), 824(m), 768(s), 675(s), 564(s), 520(s).

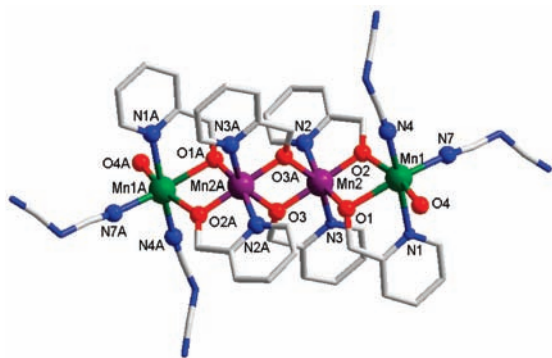


**Figure 1.** ORTEP drawing of the structure of **1**. Color scheme: Mn<sup>II</sup>, green; Mn<sup>III</sup>, purple; O, red; C, gray; N, blue. H atoms have been omitted for clarity. Symmetry code: A,  $-x, -y, -z$ .

The single-crystal X-ray diffraction analysis<sup>7</sup> reveals that **1** crystallizes in the monoclinic  $C2/c$  space group. The core of **1** consists of four Mn atoms which are arranged in a bent chain and linked by six O atoms from six hmp<sup>−</sup> ligands. Peripheral ligation is provided by six  $\eta^1:\eta^2:\mu$ -hmp<sup>−</sup>, four terminal N(CN)<sub>2</sub><sup>−</sup>, and two terminal H<sub>2</sub>O molecules. All of the Mn atoms are six-coordinated, possessing near-octahedral coordination geometries. Each of six  $\eta^1:\eta^2:\mu$ -hmp<sup>−</sup> ligands chelates one Mn ion by two donor atoms of N and O. Simultaneously, the O atom of the alkoxide arm bridges the inner neighboring Mn ions. Thus, the inner Mn atom (Mn2 or Mn2A) is coordinated by two hmp<sup>−</sup>, and the outer Mn atom (Mn1 or Mn1A) is coordinated by an hmp<sup>−</sup>, when four Mn ions are in a linear array. Around the outer Mn ions, three coordination sites are held by two N atoms of two N(CN)<sub>2</sub><sup>−</sup> and an O atom of the H<sub>2</sub>O molecule, respectively, for completion of the six-coordination configuration. The oxidation states of the Mn atoms and the protonation level of the O atoms were obtained from bond valence sum (BVS) calculations.<sup>8</sup> The results indicate that outer and inner Mn atoms are 2+ and 3+, respectively, and all Hhmp ligands are deprotonated. Moreover, Mn<sup>III</sup> ions display a Jahn–Teller (JT) distortion for a high-spin 3d<sup>4</sup> ion in near-octahedral geometry, taking the form of an axial elongation (N3–Mn2–O3A and N3A–Mn2A–O3 lie approximately parallel to each other). The intracuster Mn⋯Mn distances of Mn1⋯Mn2 and Mn2⋯Mn2A are 3.212(3) and 3.234(1) Å, respectively. The doubly bridging angles of Mn1–O1–Mn2, Mn1–O2–Mn2, and Mn2–O3–Mn2A are 101.85(15), 105.30(16), and 105.00(15)°, respectively. The angle of Mn1–Mn2–Mn2A is 126.98(3)°, indicating that the metal centers are not arranged in a straight line but with a considerable bent angle. Such a specific bridging mode may provide an opportunity to obtain interesting magnetic properties different from those of double-cubical structures containing hmp<sup>−</sup> ligands reported by others.<sup>5a</sup> The outer Mn–O/N bond distances ranged from 2.139(4) to 2.309(4) Å, whereas the inner Mn–O/N bond distances are in the

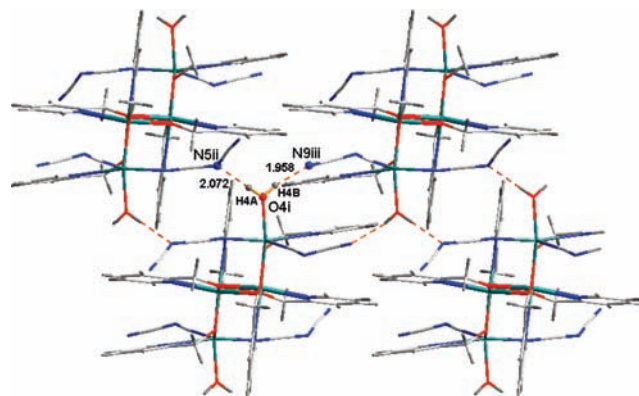


**Figure 2.** View of the interactions between discrete **1**, in which hydrogen bonds and the JT directions of the Mn<sup>III</sup> ions are shown as dashed and bold black lines, respectively. Symmetry codes: i,  $0.5 + x, 0.5 - y, 0.5 + z$ ; ii,  $0.5 - x, 0.5 - y, 1 - z$ ; iii,  $1 - x, 1 - y, 1 - z$ .

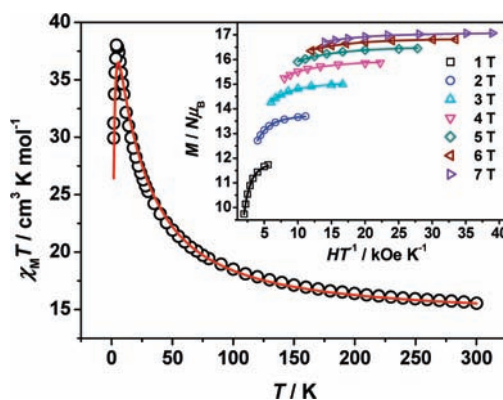


**Figure 3.** Plot of  $\chi_M T$  vs  $T$  of **1** in an applied field of 2 kOe. Inset: Plot of the reduced magnetization ( $M/N\mu_B$ ) vs  $H/T$  at the indicated applied fields. The solid lines represent the best-fit calculations.

range of 1.874(3)–2.266(4) Å. It should be noted that, to the best of our knowledge, this linear arrangement within **1** is unprecedented in tetranuclear manganese clusters.

Upon careful inspection of the structure of **1**, we find that there are intramolecular but no intermolecular  $\pi$ – $\pi$  stacking interactions in the complex. Among molecules, two kinds of significant hydrogen bonds were observed from coordinated H<sub>2</sub>O molecules to middle or terminal N atoms of N(CN)<sub>2</sub><sup>−</sup> ions (O4i⋯N5ii, 2.915(6) Å; H4A⋯N5ii, 2.072 Å and O4i⋯N9iii, 2.798(7) Å; H4B⋯N9iii, 1.958 Å), which extend the discrete Mn<sub>4</sub> clusters into a 2D framework (Figure 2).

The temperature dependence of magnetic susceptibilities for complex **1** was measured in the temperature range 1.8–300 K in a constant magnetic field of 2 kOe and is shown as  $\chi_M T$  vs  $T$  plots in Figure 3. The  $\chi_M T$  value at 300 K is 15.55 cm<sup>3</sup> K mol<sup>−1</sup>, somewhat higher than the spin-only value (14.75 cm<sup>3</sup> K mol<sup>−1</sup>) expected for magnetically isolated high-spin 2Mn<sup>II</sup> and 2Mn<sup>III</sup> ions with  $g = 2.00$ . Upon cooling,  $\chi_M T$  increases monotonically and reaches a maximum of 38.02 cm<sup>3</sup> K mol<sup>−1</sup> at 4.0 K and then abruptly decreases to 29.93 cm<sup>3</sup> K mol<sup>−1</sup> at 1.8 K, indicating an overall ferromagnetic interaction in **1**. The low-temperature decrease may be due to ZFS or Zeeman effects or both. Furthermore, the magnetic susceptibilities above 50 K can be fitted well by the Curie–Weiss law  $\chi = C/(T - \theta)$ , obtaining  $C = 14.69$  cm<sup>3</sup> K mol<sup>−1</sup> and  $\theta = 19.65$  K (Figure S1 in the Supporting

(7) Crystal data for **1**: Mn<sub>4</sub>C<sub>44</sub>H<sub>40</sub>N<sub>18</sub>O<sub>8</sub>,  $M = 1168.70$ , monoclinic, space group  $C2/c$ ,  $a = 26.24(3)$  Å,  $b = 11.313(2)$  Å,  $c = 18.768(2)$  Å,  $\beta = 117.870(3)^\circ$ ,  $V = 4925(6)$  Å<sup>3</sup>,  $Z = 4$ ,  $D_c = 1.576$  g/cm<sup>3</sup>,  $F(000) = 2376$ , crystal dimensions  $0.48 \times 0.46 \times 0.42$  mm,  $R1 = 0.0559$ ,  $wR2 = 0.1373$  for 4334 reflections with  $I > 2\sigma(I)$ ,  $GOF = 0.999$ , largest peak/hole 0.888/−0.573.

(8) (a) Liu, W.; Thorp, H. H. *Inorg. Chem.* **1993**, *32*, 4102. (b) Brown, I. D.; Shannon, R. D. *Acta Crystallogr.* **1973**, *A29*, 266. (c) Donnay, G.; Allman, R. *Am. Mineral.* **1970**, *55*, 1003.

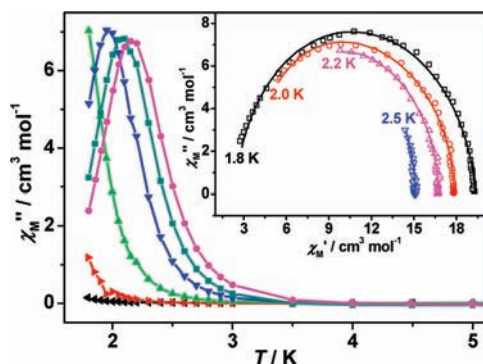


**Figure 4.** Plot of the in-phase ( $\chi_M'$ ) and out-of-phase ( $\chi_M''$ ) ac susceptibility signals for complex **1**, recorded with frequencies of 1 (black left-pointing  $\blacktriangle$ ), 10 (red right-pointing  $\blacktriangle$ ), 100 (neon-green  $\blacktriangle$ ), 499 (blue  $\blacktriangledown$ ), 997 (dark-green  $\blacksquare$ ), and 1488 (pink  $\bullet$ ) Hz. Inset: Cole–Cole diagram for **1**. The solid line represents the least-squares fit by the Debye model.

Information). According to the structure of **1**, there are two different magnetic interactions between neighboring Mn atoms, namely,  $J_1$  and  $J_2$ , representing the coupling of  $\text{Mn}^{\text{II}}/\text{Mn}^{\text{III}}$  and  $\text{Mn}^{\text{III}}/\text{Mn}^{\text{III}}$ , respectively. Therefore, the Hamiltonian of **1** can be given as

$$\mathbf{H} = -2J_1(S_{\text{Mn1}}S_{\text{Mn2}} + S_{\text{Mn1A}}S_{\text{Mn2A}}) - 2J_2S_{\text{Mn2}}S_{\text{Mn2A}}$$

The magnetic data were fitted by a least-squares fitting procedure with the Levenberg–Marquardt method using the program *MAGPACK*.<sup>9</sup> The best parameters fitted in the temperature range of 1.8–300 K are  $J_1 = 3.94 \text{ cm}^{-1}$ ,  $J_2 = 1.36 \text{ cm}^{-1}$ ,  $g = 1.95$ , and  $R = \sum[(\chi_M T)_{\text{calc}} - (\chi_M T)_{\text{obs}}]^2 / \sum(\chi_M T)_{\text{obs}}^2 = 4.52 \times 10^{-4}$ , with the result shown as the solid line in Figure 3. It is obvious that complex **1** is ferromagnetically coupled to give a  $S = 9$  ground state, with an  $S = 8$  first excited state lying  $4.03 \text{ cm}^{-1}$  above.

In order to further characterize the ground-state spin  $S$ ,  $g$  value, and ZFS parameter  $D$ , magnetization data were collected in the ranges of 1–7 T and 1.8–5.0 K, which were plotted as the reduced magnetization ( $M/N\mu_B$ ) versus  $H/T$  in the inset of Figure 3. The data were fitted by matrix diagonalization using the *ANISOFT* program,<sup>10</sup> including isotropic Zeeman interactions, axial ZFS ( $D\hat{S}_z^2$ ), and a full powder average of the magnetization, when assuming that only the ground state is populated at these temperatures and magnetic fields. The best fits are obtained with  $S = 9$ ,  $D = -0.28 \text{ K}$ , and  $g = 1.93$ . The data are well fitted, indicating that the populations of low-lying excited states at 1.8–5.0 K are low and/or the intermolecular interactions are relatively small. In addition, it should be noted that, although the sign of the fitted  $D$  parameter cannot be assured completely, its absolute value is relatively believable. The nonsuperposition of the isofield lines also indicates the presence of significant ZFS in complex **1**.

To probe the magnetization dynamics of **1**, alternating-current (ac) susceptibility studies were performed in a zero

applied dc field with a 5.0 Oe ac field oscillating at frequencies in the range of 1–1488 Hz and in the temperature range of 1.8–10.0 K. Figures 4 and S2 in the Supporting Information show the in-phase ( $\chi_M'$ ) and out-of-phase ( $\chi_M''$ ) signals versus  $T$  curves for complex **1**. The data reveal that below  $\sim 3.2 \text{ K}$  both  $\chi_M'$  and  $\chi_M''$  are strongly frequency-dependent. As the frequency ( $f$ ) of the ac field was changed from 1488 to 499 Hz, the  $\chi_M''$  peak temperature ( $T_p$ ) shifted from 2.20 to 1.95 K. A quantity given by  $(\Delta T_p/T_p)/\Delta(\log f)$  is estimated to be 0.2, which falls in the range of a superparamagnet and excludes the possibility of a spin glass.<sup>11</sup> The Arrhenius equation of  $\tau = \tau_0 \exp(\Delta E_{\text{eff}}/k_B T)$  (where  $\tau = 1/2\pi f$ ,  $\Delta E_{\text{eff}}$  is the effective energy barrier for the magnetization relaxation, and  $\tau_0$  is the preexponential factor) was employed to extract parameters relevant to a slow magnetic relaxation. The results show that there is a linear correlation of  $1/T_p$  versus  $\ln(2\pi f)$  and the parameters are  $\Delta E_{\text{eff}} = 16.24 \text{ K}$  and  $\tau_0 = 2.0 \times 10^{-9}$  (Figure S3 in the Supporting Information). Moreover, the Cole–Cole plot of the in-phase ( $\chi_M'$ ) versus out-of-phase ( $\chi_M''$ ) signals of the ac magnetic susceptibility of **1** exhibits a semicircular shape (inset of Figure 4), which was well fitted by a Debye model to give an  $\alpha$  parameter of 0.04–0.09, indicative of a narrow distribution of the relaxation times necessary for SMM behavior.<sup>12</sup> It should be noted that the  $D$  values for **1** are similar to other hmp<sup>−</sup>-containing  $\text{Mn}_4$  clusters (which are usually found around 0.2–0.3 K).<sup>5a</sup> To the best of our knowledge, their similar  $D$  values may result from a similarly parallel arrangement of the JT axes of the only two  $\text{Mn}^{\text{III}}$  ions. Moreover, complex **1** and other hmp<sup>−</sup>-containing  $\text{Mn}_4$  clusters possess  $S = 9$  ground states; therefore, their  $\Delta E_{\text{eff}}$  values are also similar.<sup>5a</sup>

In summary, we have synthesized a new linear tetranuclear manganese cluster via self-assembly. The magnetic investigation indicates that complex **1** is a SMM. To the best of our knowledge, complex **1** is a rare SMM representing a linear molecular structure.

**Acknowledgment.** We thank to the National Natural Science Foundation of China (Grants 20671048 and 20771057), Major State Basic Research Development Program (No. 2007CB925102), and Shandong “Tai-Shan Scholar Research Fund” for financial support.

**Supporting Information Available:** Experimental procedures, plot of  $\chi_M^{-1}$  vs  $T$ , plots of in-phase signals versus temperature, plot of  $\ln(2\pi f)$  vs  $T_p^{-1}$ , plots of  $\chi''$  vs frequencies, and a table of BVS calculations. This material is available free of charge via the Internet at <http://pubs.acs.org>. Crystallographic data for the structural analysis of the compounds have been deposited with the Cambridge Crystallographic Data Centre, under CCDC no. 655607. Copies of this information may be obtained free of charge from The Director, CCDC, 12 Union Road, Cambridge CB2 1EZ, U.K. (<http://www.ccdc.cam.ac.uk>; fax +44-1223-336033).

(9) (a) Borrás-Almenar, J. J.; Clemente-Juan, J. M.; Coronado, E.; Tsukerblat, B. S. *Inorg. Chem.* **1999**, *38*, 6081. (b) Borrás-Almenar, J. J.; Clemente-Juan, J. M.; Coronado, E.; Tsukerblat, B. *J. Comput. Chem.* **2001**, *22*, 985.

(10) Shores, M. P.; Sokol, J. J.; Long, J. R. *J. Am. Chem. Soc.* **2002**, *124*, 2279.

(11) (a) Mydosh, J. A. *Spin Glasses: An Experimental Introduction*; Taylor & Francis: London, 1993. (b) Wang, S.; Zuo, J.-L.; Gao, S.; Song, Y.; Zhou, H.-C.; Zhang, Y.-Z.; You, X.-Z. *J. Am. Chem. Soc.* **2004**, *126*, 8900–8902.

(12) (a) Cole, K. S.; Cole, R. H. *J. Chem. Phys.* **1941**, *9*, 341. (b) Lopez, N.; Prosvirnin, A. V.; Zhao, H. H.; Wernsdorfer, W.; Dunbar, K. R. *Chem.—Eur. J.* **2009**, *15*, 11390.